Published in final edited form as:
J Immunol. 2013 July 15; 191(2): 773–784. doi:10.4049/jimmunol.1300113.

Microenvironments in tuberculous granulomas are delineated by distinct populations of macrophage subsets and expression of nitric oxide synthase and arginase isoforms

Joshua T. Mattila[*], **Olabisi O. Ojo**[*], **Diane Kepka-Lenhart**[*], **Simeone Marino**[†], **Jin Hee Kim**[‡], **Seok Yong Eum**[§], **Laura E. Via**[¶], **Clifton E. Barry III**[¶], **Edwin Klein**[‖], **Denise E. Kirschner**[†], **Sidney M. Morris Jr**[*], **Philana Ling Lin**[#], and **JoAnne L. Flynn**[*,**]

[*]Department of Microbiology and Molecular Genetics, University of Pittsburgh, Pittsburgh, PA 15261

[†]Department of Microbiology and Immunology, University of Michigan Medical School, Ann Arbor, MI

[‡]National Masan Tuberculosis Hospital, Changwon, Republic of Korea

[§]International Tuberculosis Research Institute, Changwon, Republic of Korea

[¶]Tuberculosis Research Section, Laboratory of Clinical Infectious Disease, National Institute of Allergy and Infectious Disease, National Institutes of Health, Bethesda, MD 20892

[‖]Division of Laboratory Animal Resources, University of Pittsburgh, Pittsburgh PA 15261

[#]Department of Pediatrics, Children's Hospital of Pittsburgh of the University of Pittsburgh Medical Center, Pittsburgh PA 15224

[**]Center for Vaccine Research, University of Pittsburgh School of Medicine, Pittsburgh, PA 15261

Abstract

Macrophages in granulomas are both anti-mycobacterial effector and host cell for *Mycobacterium tuberculosis*(*M.tb*), yet basic aspects of macrophage diversity and function within the complex structures of granulomas remain poorly understood. To address this, we examined myeloid cell phenotypes and expression of enzymes correlated with host defense in macaque and human granulomas. Macaque granulomas had upregulated inducible and endothelial nitric oxide synthase (iNOS and eNOS) and arginase (Arg1 and Arg2) expression and enzyme activity compared to non-granulomatous tissue. Immunohistochemical analysis indicated macrophages adjacent to uninvolved normal tissue were more likely to express CD163, while epithelioid macrophages in regions where bacteria reside strongly expressed CD11c, CD68 and HAM56. Calprotectin-positive neutrophils were abundant in regions adjacent to caseum. iNOS, eNOS, Arg1 and Arg2 proteins were identified in macrophages and localized similarly in granulomas across species, with greater eNOS expression and ratio of iNOS:Arg1 expression in epithelioid macrophages, as compared to cells in the lymphocyte cuff. iNOS, Arg1 and Arg2 expression in neutrophils was also identified. The combination of phenotypic and functional markers support that macrophages with anti-inflammatory phenotypes localized to outer regions of granulomas while the inner regions were more likely to contain macrophages with pro-inflammatory, presumably bactericidal, phenotypes. Together these data support the concept that granulomas have organized

Corresponding author: JoAnne Flynn, W1144 Biomedical Science Tower, 200 Lothrop Street, University of Pittsburgh School of Medicine, Pittsburgh, PA 15261; joanne@pitt.edu; phone: 412.624.7743; FAX: 412.383.7220.

Competing financial interests: The authors declare no competing financial interests.

microenvironments that balance anti-microbial anti-inflammatory responses to limit pathology in the lungs.

Introduction

The initial immunologic events following *Mycobacterium tuberculosis*(*M.tb*) infection include cytokine- and chemokine-mediated recruitment of monocytes, neutrophils and tissue-resident macrophages (1). Macrophages alone are not sufficient to control intracellular replication in the majority of cases but must interact with activated T cells (2). The product of these interactions is the granuloma, an organized structure rich in macrophages and lymphocytes that acts as a functional unit for controlling *M.tb* infection. The presence of granulomas is not necessarily indicative of controlled *M.tb* infection since hosts with active TB have numerous granulomas, but the fact that most *M.tb*-infected individuals never experience active disease (1) suggests that granulomas in immunologically-competent individuals can be highly effective at restraining bacterial growth and dissemination.

The necrotic (caseous) granuloma is the most common lesion associated with active TB. Necrotic granulomas have an outer “lymphocyte cuff” dominated by T and B cells, and a macrophage-rich middle region that surrounds an amorphous center of caseous necrosis. Other types of granulomas include completely cellular, non-necrotic granulomas and suppurative granulomas (heavily infiltrated by neutrophils) (3). In experimentally infected cynomolgus macaques, caseous granulomas form by 4-6 weeks post infection (4, 5), while non-necrotic granulomas are not observed until later and primarily during active or reactivated disease (5). Partially mineralized and highly fibrotic (fibrocalcific) granulomas are associated with clinically latent infection but can also be found in active TB. Other granuloma types, including caseous granulomas, can be present in latent infection as well, indicating that the “types” of granulomas that are present incompletely describe the infection status of the host. This being said, latent *M.tb* infection is associated with lower numbers of granulomas than active TB (6).

The high level of stratification in human and nonhuman primate granulomas (3, 7) suggests that protection depends on microenvironments (8, 9) that promote bacterial clearance while minimizing damage to uninvolved tissues adjacent to the granuloma. Macrophage subsets engaging in anti-inflammatory or pro-inflammatory processes are likely to be important, yet poorly understood, mediators determining the characteristics of these microenvironments. Activated macrophages are often classified as either classically-activated M1 (pro-inflammatory) macrophages that engage in bactericidal activity or alternatively-activated M2 (anti-inflammatory) macrophages that mediate pro-healing responses. Expression of inducible nitric oxide synthase (iNOS) is the hallmark of pro-inflammatory macrophages, and in murine systems, is necessary for improved resistance to TB (10-12). iNOS-expressing macrophages have been identified in the lungs of humans with TB (13-15) although a correlation between human TB and deficient iNOS expression has proven difficult (16). The other NOS isoforms, endothelial NOS (eNOS) and neural NOS (nNOS), can also be present in granulomas (13) but it is not known whether they have homeostatic or bactericidal functions.

Pro-healing anti-inflammatory macrophages are characterized by arginase 1 (Arg1) expression (17, 18), although this is best defined in murine systems. Arginases can compete with nitric oxide synthases for L-arginine and generate urea and L-ornithine, which can be subsequently converted to L-proline (19), an amino acid used in collagen synthesis and wound healing (20, 21), or to polyamines (19), which can play a variety of roles in cell physiology and pathophysiology (22). While anti-inflammatory macrophages have

important functions in healing and anti-helminth responses (23), arginase expression can diminish protection against intracellular pathogens, including *M.tb*(24, 25). Macrophage arginase expression has been identified in tuberculous lung from humans (26) and also in peripheral blood mononuclear cells of patients infected with *M.tb*(27) but the contribution of arginase to protective or pathologic responses in *M.tb* infection in humans remains undetermined. The NOS/arginase paradigm of macrophage activation is best defined for mice, however, and the signals in primates that drive macrophage activation remain largely undefined. Considering this, it is likely that macrophage polarization occurs on a spectrum (28) with classical and alternative activation on opposing ends of a spectrum but with most macrophages having characteristics somewhere along that continuum.

We examined granulomas from cynomolgus macaques with active or clinically latent *M.tb* infection to determine whether specific populations of macrophage localize to specific microenvironments in different granuloma types. Moreover, because NOS and arginase expression may mediate anti-mycobacterial activity and immunopathology, we sought to identify how NOS and arginase expression relates to the distribution of microenvironment-specific macrophage populations. Studies using mathematical modeling have suggested that granulomas are organized in a non-random fashion, and chemokine and cytokine gradients also exist, helping to establish cell patterns (29). We present biochemical, molecular and immunohistochemical evidence demonstrating that macrophages and neutrophils in macaque granulomas can express functional NOS and arginase enzymes and are organized into different microenvironments. Furthermore, we identified similarities in macrophage distribution and NOS and arginase expression between macaque and human granulomas, suggesting these functions are conserved across primate species. These results provide new data on the diversity of macrophages and neutrophils in granulomas and their effector capacity and thus may lead to an improved understanding of the mechanisms underlying anti-mycobacterial responses.

Materials and Methods

Tissue processing and sectioning

All animal procedures and husbandry practices were included in protocols approved by the University of Pittsburgh's Institutional Animal Use and Care Committee (IACUC). Cynomolgus macaques were infected with low dose (~25 CFU) Erdman-strain *M.tb* as previously described (4). Macaques with active TB were humanely euthanized and necropsied as previously described (4, 5). All samples obtained were from animals undergoing necropsy as part of other studies. For immunohistochemistry, granuloma containing-tissues were excised and fixed in 10% neutral buffered formalin prior to placement in histology cassettes and paraffin embedding. Tissues were cut into 5 μm-thick sections by the University of Pittsburgh Medical Center's *in situ* histology lab and mounted on SuperFrost Plus slides (Thermo Fisher Scientific, Waltham, MA). Formalin-fixed paraffin-embedded human lung tissue samples containing granulomas were dissected from tissue removed during therapeutic lung resection surgery at the National Masan Tuberculosis Hospital (NHTH) from patients refractory to second line drug therapy. Tissue collection (2003-2007) was approved by the NMTH institutional review board, an exemption from NIH, and with written consent of the subjects; samples were de-identified when provided for analysis.

Immunofluorescence, Immunohistochemistry, imaging and image analysis

Formalin-fixed paraffin-embedded tissue sections from *M. tuberculosis*-infected macaques m907, m9209 m1307, m1707, m3809, m9905, m10708, m21802, m15304, and m13207 were selected for study. All animals except m10708 had active TB at the time of necropsy.

Tissue sections were deparaffinized in xylene, 100% ethanol, and 95% ethanol. Tissue sections were then placed into an antigen retrieval buffer (20 mM Tris/820 μM EDTA/ 0.00005% Tween 20 [pH 9.0]) containing pressure cooker (Manttra, Piscataway, NJ), incubated under pressure for 7 minutes before removal from the hotplate and allowed to cool slowly over 30 minutes. Sections were incubated in blocking buffer (2.5% BSA in PBS) for 30 minutes at 37°C, prior to addition of primary antibody diluted in blocking buffer. Antibodies for immunohistochemistry were against human CD3ε (ready-to-use format, 1:2 dilution; Dako, Carpintera, CA), CD11c (clone 5D11, 1:30 dilution; Leica Microsystems, Buffalo Grove, IL), CD68 (clone KP1, 1:50 dilution; Labvision, Freemont, CA), CD163 (clone 10D6, 1:30 dilution; Labvision), calprotectin (clone MAC387, 1:100 dilution; Labvision), HAM56 (ready-to-use format, 1:2 dilution; Enzo Life Sciences, Farmingdale, NY), iNOS (rabbit polyclonal; Labvision), eNOS (rabbit polyclonal; Labvision), arginase 1 (clone 19/arginase1, 1:100 dilution; BD Bioscience), arginase 2 (rabbit polyclonal, 1:40 dilution; Santa Cruz Biotechnology, Santa Cruz, CA), nitrotyrosine (rabbit polyclonal, 1:100 dilution; Millipore, Billerica, MA). The specificity of iNOS and eNOS antibodies were confirmed by western blotting of iNOS and eNOS (0.1 ug/lane) in conjunction with 1 ug of *M.tb* lysate to confirm that the antibodies were isoform-specific and not reactive with bacterial proteins (data not shown). We were unable to identify an anti-nNOS antibody that worked for immunohistochemistry in macaque tissues and was not cross-reactive with other NOS isoforms (data not shown). Tissue sections were incubated at room temperature in cocktails of primary antibodies for 1 hr. Secondary antibodies, purchased from either Jackson ImmunoResearch Laboratories (West Grove, PA) or Life Technologies, were diluted in blocking buffer and applied to tissue sections that had been washed 3-5 times with IHC wash buffer (0.2% Tween-20 in PBS) and incubated for 1 hr at room temp in the dark. HAM56 was stained with an anti-mouse μ-chain specific secondary antibody (Jackson ImmunoResearch) that was made in donkey and not crossreactive with mouse IgG antibodies. The specificity of secondary antibodies was confirmed either by isotype or no-primary controls using the same staining and imaging protocol as sections containing stained with primary antibodies. The slides were then washed 3-5 times with IHC buffer and directly-labeled conjugates applied. Antibodies for direct labeling were chosen based on their ability to work well following significant dilution when used with a secondary antibody. The unlabeled antibodies were labeled with either Alexa Fluor 488 or Alexa Fluor 647 using the Zenon direct labeling kit (Life Technologies). Tissue sections were incubated with direct conjugates for 2 hrs at room temperature or overnight at 4°C. Slides were washed 4 times with IHC wash buffer, once with PBS and then coverslips were applied using Prolong Gold mounting medium containing DAPI (Life Technologies). Slides were cured for 24 hours at room temperature before imaging. Granulomas were imaged with either an Olympus Fluoview 500 or Fluoview 1000 laser scanning confocal microscope (Olympus, Center Valley, PA) maintained by the University of Pittsburgh's Center for Biologic Imaging and a Fluoview 1000 laser scanning confocal microscope maintained by the University of Pittsburgh's Microbiology and Molecular Genetics Department. Individual tissue sections from animals with active TB frequently contained multiple granulomas of various sizes and type; we chose to image granulomas with features that were representative of that particular granuloma type. Three color images (red, green, far red [pseudocolored as blue]) were acquired sequentially, followed by a DAPI image (gray) showing nuclei. Images (either single sections or serial z sections acquired at 1 μm intervals) were acquired and saved as TIFF-format images. Z series images were opened with MacBiophotonics ImageJ [available at http://www.macbiophotonics.ca/downloads.htm] or FIJI [available at http://pacific.mpi-cbg.de/wiki/index.php/Downloads] and saved as maximum intensity projections. At least three fields in the macrophage-lymphocyte region were imaged at 400-600x magnification for counting cells in tissues. Images were opened in Photoshop CS4 (Adobe Systems, San Jose CA), overlaid with a grid to facilitate analysis and counted manually by examining each channel separately or in combination for positively-stained

cells. The number of nuclei per image, which was used to determine the number of cells within an image, was assessed with CellProfiler v2.0 [available at http://www.cellprofiler.org/]. Granulomas were too large to be imaged by one 200x field; consequently, multiple overlapping fields were acquired and the image of the entire granuloma assembled into a single montage using Photoshop. Preliminary work indicated that counting individual cells in granulomas for phenotypic analysis by automated or manual means was not going to be feasible due to the complexity of the environment, consequently, we used a region-based approach to analyze staining (signal) intensity in lymphocyte cuff or epithelioid macrophage regions. For analysis of region-based characteristics (macrophage markers, iNOS/Arg1 expression), non-overlapping image fields (200x magnification) of granulomas containing both epithelioid macrophage and lymphocyte cuff regions were acquired as previously indicated. From these images, regions of interest were drawn around epithelioid macrophage or lymphocyte cuff regions and the mean pixel intensity of the red, green, and blue channels was determined with Photoshop's histogram tool. The iNOS:Arg1 ratio was calculated by dividing the mean iNOS signal by the mean Arg1 signal. Pairwise comparisons were made between macrophage surface marker signal or iNOS:Arg1 signal ratio were made between the epithelioid macrophage and lymphocyte cuff regions.

Auramine-rhodamine staining

Granulomas were stained with auramine-rhodamine reagents to visualize the mycobacterial cell wall component mycolic acid. Tissue sections were deparaffinized as previously indicated and equilibrated in dH_2O for 5 minutes before being stained with auramine-rhodamine for 30 minutes. Excess stain was washed off with dH2O and decolorized in multiple washes of isopropanol with 5% HCl (v/v) before being counterstained with potassium permanganate for 50 seconds. Slides were washed and air dried before imaging. All auramine-rhodamine staining reagents were purchased from BD Bioscience. Auramine-rhodamine-stained slides were imaged on an Olympus Provis epifluorescence microscope at 200x magnification. Following this, the immersion oil was removed in a xylene bath and the slides were then stained with hematoxylin and eosin (H&E) using standard protocols. Coverslips were mounted on H&E-stained slides with Permount (Thermo Fisher Scientific) and the same tissue section used for the auramine-rhodamine staining was used to acquire the H&E image on the same microscope previously used to ensure consistent magnification and perspective. To determine the localization of *M.tb* or *M.tb* antigens in granulomas and colocalize them with cells, the red auramine-rhodamine image was overlayed on a grayscale image of the H&E-stained granuloma with Photoshop, and this position located on the color version of the H&E.

NOS and arginase activity assays

Granuloma-containing tissues for arginase assays that had been flash frozen in liquid nitrogen at necropsy and stored at -80°C were homogenized with a Medimachine tissue homogenizer (BD Biosciences) under BSL3 conditions. Tissues were homogenized in PBS containing 0.1% Triton-X-100 and protease inhibitor cocktail (Thermo Fisher Scientific) without EDTA and filtered through a 0.22 μm syringe filter. Protein concentrations were measured using a BCA Protein Assay Kit (Thermo Fisher Scientific) with BSA as a protein standard. Arginase or NOS activity were assayed under BSL2 conditions using filter-sterilized samples. Arginase activity was determined as previously described (30) by following the conversion of L-[guanidino-^{14}C]arginine to [^{14}C]urea, which was quantified by scintillation counting after its conversion to $^{14}CO_2$ and trapping as $Na_2{}^{14}CO_3$. Tissues for NOS assays were from recently necropsied animals that had been homogenized (see below) and stored at -80°C until the time of assay. Initial attempts to quantify NOS activity in lung homogenates was done using the [^{3}H]L-arginine to [^{3}H]citrulline conversion-based assay but yielded unacceptable levels of background signal that was not inhibited by selective

NOS or arginase inhibitors. Consequently, NOS activity was determined using a cell lysate-based assay that measured nitrite (NO_2^-) via the Griess reaction. Lung tissue was homogenized and lysed in 1-3 mL of 25 mM Tris-HCl [pH 7.4] with 1 mM EDTA and 1 mM EGTA and filter sterilized by passing through a 0.22 μm syringe filter. Protein concentrations in tissue homogenates were measured by BCA protein assay (Thermo Fisher Scientific). NOS assays were performed by adding 10 μL of tissue homogenate to 40 μL of assay buffer (75 μM L-arginine, 1 mM NADPH, 0.25 μM calmodulin, 2.5 mM FAD, 2.5 mM FMN, 10 μM tetrahydrobiopterin, 440 μM nor-NOHA [Cayman Chemical Company, Anne Arbor, MI], 120 μM $CaCl_2$, 120 μM $MgCl_2$ in 100 mM HEPES) followed by an overnight incubation at 37°C to ensure the reaction went to completion. A replicate control sample was prepared in the same buffer but included N6-(1-iminoethyl)-L-lysine, (L-NIL; Cayman Chemical Company), a selective iNOS inhibitor. Recombinant nitrate reductase was added to the reaction to convert nitrate to nitrite and then the reaction assayed with freshly-prepared Griess reagent (0.05% naphthylethylenediamine dihydrochloride and 0.5% sulfanilamide in 2.5% H_3PO_4) on a plate reader (Molecular Devices, Sunnyvale, CA) with a standard curve prepared from nitrite-containing homogenization buffer. Data were analyzed by measuring the concentration of nitrite (based on the standard curve) in the uninhibited and L-NIL inhibited samples. Two factors were taken into consideration in the data analysis: the intrinsic coloration of the homogenate imparted by hemoglobin and significantly different protein concentrations related to differences in the size of tissues that were homogenized. To account for these factors, we divided the measured nitrite concentration in the uninhibited sample by the measured nitrite concentration in the L-NIL inhibited control to determine the % of control, and then this value was divided by the mass of protein per assay. Normalized data are expressed as % of control/μg protein. Unless otherwise noted, reagents were purchased from Sigma Aldrich.

Quantitative real time PCR

RNA was obtained from 8 *M.tb* culture-positive (involved) and 4 culture-negative (uninvolved) tissues from m907, m1307, m1707, m9803, m16705, m13207, m10403 and m16705 stored in RNAlater (Life Technologies, Grand Island, NY) at −80°C at necropsy. Tissues were disrupted in Trizol (Life Technologies) under BSL3 conditions and RNA was isolated using a standard phenol-chloroform isolation followed by cleanup with RNeasy columns (Qiagen, Valencia, CA). RNA was quantified on a DU-800 spectrophotometer (Beckman Coulter, Brea, CA) and used for quantitative reverse transcription PCR (qRT-PCR). Arg1 (HP200032) and Arg2 (HP205107) primers were purchased from Origene (Rockville, MD) while eNOS primers were purchased from Realtimeprimers.com (Elkins Park, PA). iNOS (fw: TCTTGGTCAAAGCTGTGCTC; rev: CATTGCCAAACGTACTGGTC) and nNOS (fw: TAGCTTCCAGAGTGACAAAGTGACC; rev: TGTTCCAGGGATCAGGCTGGTATTC) primers were based on the respective human RNA sequences and the identity of the product confirmed by sequencing. HPRT mRNA (fw: TTACCTCACTGCTTTCCGGAG; rev: AGTCTGGCTTATATCCAACAT) was quantified as an internal control. Unless otherwise indicated, primers were purchased from Sigma-Aldrich. Amplification was performed on an iCycler (Bio-Rad, Hercules, CA) using AMV reverse transcriptase (Promega, Madison, WI) and GoTaq qPCR Master Mix reagents (Promega). Samples were assayed in duplicate for each tissue. Relative quantification based on the ΔΔCt method (31) with HPRT (also performed in duplicate) used as a housekeeping control.

Flow cytometry to identify calprotectin as a neutrophil marker

Whole blood from macaques was isolated as previously described (32). Preliminary experiments demonstrated that percoll gradient isolation of PBMCs from whole blood separates cells into two fractions, a lymphocyte and monocyte-rich fraction and a neutrophil

and RBC-rich fraction. Neutrophils in the RBC fraction had physical characteristics that did not differ from neutrophils in RBC-lysed whole blood. Neutrophils from the RBC pellet were stained after lysing the RBCs with PharmLyse (BD Biosciences) and the cells fixed and permeablized with the Cytofix/Cytoperm and Perm/Wash buffers (BD Biosciences) for intracellular antigen staining. Cells were stained for CD163 (clone eBioGHI/61; eBiosciences, San Diego, CA) and calprotectin (clone MAC387; Labvision, San Diego, CA) that had been labeled with the Zenon labeling kit (Life Technologies). Cells phenotypes were read using an LSRII flow cytometer (BD Bioscience).

Data analysis and statistics

Data were analyzed with Graph Pad Prism 5.0 (Graph Pad software, La Jolla, CA). Comparisons between treatments were made using the nonparametric Mann-Whitney test and pairwise comparisons between granuloma regions were made using the nonparametric Wilcoxon matched-pairs signed rank test with $p<0.05$ considered statistically significant. Flow cytometric data was analyzed using the FlowJo software package (Treestar Inc, Ashland, OR).

Results

Arg1, Arg2, iNOS, and eNOS are expressed and functional in the granuloma

Factors initiating macrophage polarization and phenotypes of classically or alternatively activated macrophages have not been fully resolved in primates. In mice, nitric oxide synthase expression defines classically-activated macrophages while arginase expression delineates alternatively-activated macrophage populations, consequently, we used Arg1, Arg2, iNOS or eNOS (Figure 1) as markers for macrophage function with the caveat that these markers may not fully describe macrophage polarization. Moreover, because of the difficulty assigning an activation state to primate macrophages, we will use the term ‘pro-inflammatory’ to indicate macrophages with dominant NOS expression and ‘anti-inflammatory’ to characterize macrophages with dominant arginase expression. Arg1 was abundant in macrophages while the most intense Arg2 signal occurred as discrete granules in cells with segmented nuclei and at much lower levels in macrophages (Figure 1A). iNOS and eNOS were identified in macrophages, each with a characteristic staining pattern. Macrophage iNOS had a punctate appearance and appeared to be scattered throughout the cytoplasm (Figure 1A) while eNOS staining in epithelioid macrophages was more intense and associated with the cell membrane (Figure 1A). We also found substantial iNOS and Arg1 co-expression, particularly in macrophages (Figure 1B) but also in neutrophils (Figure 1B). These results demonstrate that macrophage activation is not binary but occurs along a spectrum.

Real time reverse transcription PCR (qRT-PCR) and biochemical assays for arginase and NOS activity confirmed that arginase and NOS are expressed and functional in granulomas. qRT-PCR indicated *Arg1*, *Arg2*, *eNOS* and *iNOS* expression was upregulated in granuloma-containing tissues relative to uninfectedcontrol tissues (Figure 2A), with *Arg1* and *iNOS* upregulated more than *Arg2* and *eNOS*, respectively. While *nNOS* expression was identified, its expression in granulomas was not strongly upregulated above uninfected lung. Biochemical assays for enzyme activity in tissue lysates demonstrated that granuloma-containing tissues had significantly more arginase and NOS activity than uninvolved tissues (Figure 2B-2D). The NOS activity associated with individual granulomas within a monkey was highly variable but generally higher than the NOS activity from uninvolved lung from that same monkey (Figure 2C). When these data were aggregated and compared, granulomas showed significantly more NOS activity than uninvolved tissue from infected animals (Figure 2D). Although the iNOS activity of many granulomas was inhibited by L-

NIL, it was not possible to inhibit the NOS activity in some tissues, suggesting other NOS isoforms contribute to NO production (data not shown). Finally, we identified nitrotyrosine, the nitrosylated tyrosine residues produced after NO-protein interactions, in granuloma macrophages and neutrophils (Figure 2E), supporting that the NOS species present in granulomas are functional.

Identification of macrophage- and neutrophil-specific antibodies for cynomolgus macaques

Despite the abundance of macrophages in granulomas, little is known about their molecular identities. Two categories of macrophages found in human granulomas are described morphologically (33) as epithelioid macrophages and foamy macrophages. Epithelioid macrophages are defined by their high cytoplasm:nucleus ratios and diffusely eosinophilic cytoplasm (34, 35) and are particularly abundant in granuloma regions adjacent to caseous necrosis. Foamy macrophages are also associated with tuberculous granulomas and are identifiable by their foamy, lipid-rich cytoplasm (2). To better characterize the presence and location of these cells in granulomas, we used antibodies against human macrophage antigens that we validated for use in macaque tissues. These antigens, including CD11c, CD68, CD163, HAM56 and calprotectin (Mac387), reliably stained cells in macaque tissues while we excluded other commonly used macrophage markers, including CD11b and CD14 because of their broad myeloid cell expression. DC-SIGN (CD209), a marker associate with dendritic cells, was expressed by macrophages in throughout granulomas (data not shown), and consequently, was not included in this study. We also excluded F4/80, a commonly used macrophage marker in murine systems because the human homolog (EMR1) is an eosinophil-associated protein (36) and CD15, a marker for human neutrophils because it expression on a subset of lymphocytes and lung epithelial cells (data not shown). These antibodies can react with other structures (e.g. HAM56 and CD163 with endothelium, and CD68 with fibroblasts), but endothelium is not abundant in granulomas and fibroblasts associated with granulomas did not stain positively for CD68; data not shown). Staining patterns for CD11c+, CD68+, CD163+ and HAM56+ cells were morphologically consistent with macrophage-like cells (Supplemental Figure 1). The antibody Mac387 is often described as a macrophage marker, yet in cynomolgus macaques the morphology of calprotectin-expressing cells was more neutrophil-like. Subsequent experiments identified calprotectin-bright cells in cynomolgus macaques as neutrophils (Supplemental Figure 2).

Myeloid cell populations in macaque and human granulomas

Here we imaged granulomas representing the types commonly seen in cynomolgus macaques (6) with active TB to determine whether different, antigenically-defined populations of macrophages exist in different microenvironments and how the position of these cells correlate with bacterial localization. In addition to markers of different macrophage populations, we examined the NOS and arginase expression by region to determine how microenvironments correlate with macrophage function. Macrophage activation states in primates are complex and poorly understood, so while these markers may reflect a functional capacity, we realize they cannot fully describe the full spectrum of macrophage polarization. We also imaged fibrocalcific granulomas associated with clinically latent TB to compare the organization and population structure of macrophage subsets in healed lesions with active lesions from animals that poorly controlled TB. To compare the non-human primate data with human data, we obtained de-identified samples from patients undergoing lung resection for recalcitrant TB; these patients are likely to have had long courses of infection and may have undergone several rounds of treatment. Under these circumstances, the pathology can be more complex than in macaques and can include extensive fibrosis. In fact, lung tissue samples obtained contained multiple granulomas that were often highly fibrotic; we selected non-necrotic and necrotic granulomas with the lowest

amount of fibrosis for imaging and were mindful that these lesions represent those from chronic, poorly-controlled disease hosts.

Non-necrotic granulomas

Non-necrotic granulomas were characterized by dense macrophage populations without necrotic areas (Figure 3A). CD68+ and CD163+ macrophages were most abundant at the periphery, although macrophages with lower expression of these markers could be found throughout these granulomas (Figure 3B, 3D). Neutrophils were randomly distributed throughout non-necrotic granulomas (Figure 3B). HAM56+ foamy macrophages were present but were especially abundant in central regions of granulomas with higher levels of organization (Figure 3B). The position of iNOS+ cells was similar to that observed for HAM56 expression; less organized non-necrotic granulomas had randomly distributed iNOS expression (Figure 3C) while increasingly organized granulomas had foci of iNOS expression that was consistent with the position of epithelioid macrophages (data not shown). Similarly, eNOS expression most strongly correlated with the presence and location of epithelioid macrophages (Figure 3D). Arg1-expressing cells were identified but did not localize to any particular region in these granulomas. Relatively few Arg2-expressing cells were identified, and most of these appeared to be in macrophages at the granuloma's outer edge and in neutrophils dispersed throughout the granuloma (Figure 3E).

Caseous necrotic and suppurative granulomas

Necrotic and suppurative granulomas (Figure 4) have similar features (e.g. well-defined lymphocyte cuffs and epithelioid macrophage-rich regions), but caseous granulomas have non-cellular necrotic centers and suppurative granulomas have centers nearly completely infiltrated by neutrophils. While we consider necrotic and suppurative granulomas to be defined morphotypes, they are grouped together here because of their similarities.

CD163+ macrophages were most abundant in peripheral regions of granulomas adjacent to, or inside, the lymphocyte cuff (Figure 4B, 4G, 5A, 5D). Clusters of strongly CD11c +CD68+CD163+ alveolar macrophage-like cells were often immediately adjacent to the lymphocyte cuff (Figure 5A, arrowheads). Epithelioid macrophages were CD163- or $CD163^{dim}$ but often strongly expressed CD68 (Figure 4D, 4I, 5A, 5C) and CD11c (Figure 5B). HAM56+ foamy macrophages were most abundant on the rim of the caseous or neutrophilic center (Figures 4B, 4G) with more elongate cellular morphology extending perpendicular to the center of the granuloma. Calprotectin+ neutrophils were present in the lymphocyte cuff and macrophage-rich regions but were most abundant in areas near the HAM56+ foamy macrophages adjacent to the caseum (Figure 4B) and centers of suppurative granulomas (Figure 4G). Arg1 expression was observed throughout the cellular regions of granulomas (Figure 4C, 4H) but was most strongly expressed by cells in the lymphocyte cuff (Figure 5F). Epithelioid macrophages and lymphocyte cuff macrophages also expressed iNOS (Figure 4C, 4H, 5E) with more iNOS signal observed in lymphocyte cuff region. The lymphocyte cuff region is significantly more cellular than the epithelioid macrophage region (mean density = 6373 nuclei/mm^2 vs 4459 nuclei/mm^2, respectively, p=0.0008, Mann-Whitney test, n=9 granulomas) and contains a residual population of epithelial cells that are iNOS rich, consequently this figure may over represent macrophage iNOS expression in the lymphocyte cuff region. When the ratio of iNOS:Arg1 signal intensity from epithelioid macrophages and lymphocyte cuff regions was calculated, epithelioid macrophages expressed significantly more iNOS relative to Arg1 than cells in the lymphocyte cuff region (Figure 5G), suggesting that Arg1 expression differentiates NO-generating capacity of macrophages in the epithelioid macrophage and lymphocyte cuff regions.

Strong eNOS expression was also noted in epithelioid macrophages, with the majority of eNOS associated with the plasma membrane (Figure 4D, 4I). We also observed smaller cells in the lymphocyte cuff that were strongly positive for cytoplasmic eNOS but did not stain for either macrophage or endothelial markers (CD31, Von Willebrand Factor; data not shown). Arg2 expression was largely associated with neutrophils at the border of the caseum and in the center of suppurative granulomas (Figure 4E, 4J).

Fibrocalcific granulomas

Small numbers of fibrocalcific granulomas are commonly found in latently infected hosts, but also in active TB, and are likely to represent the successful outcome of an effective immune response. These granulomas commonly contain mineralized material surrounded by fibrotic tissue and limited numbers of lymphocytes and macrophages (Figure 6A). Many of the cells in the fibrotic region surrounding mineralized centers expressed CD163 (Figure 6B). These granulomas contained very few neutrophils (Figure 6B), HAM56+ (Figure 6B) and CD68+ (Figure 6D) macrophages or eNOS-expressing macrophages (Figure 6D). iNOS and Arg1 were expressed in the cells closest to the mineralized material (Figure 6C). Arg2 expression was minimal, but strong signal was noted at the fibrosis-mineral interface (Figure 6E).

Bacteria are present in multiple areas in the granuloma

The localization of bacterial populations is poorly understood for primate granulomas. We stained granulomas for the presence of mycobacterial cell wall components with auramine-rhodamine with overlayed hematolylin and eosin-stained features to correlate the positions of bacteria and different macrophage populations. Ongoing studies in our laboratory where homogenized granulomas are plated for bacterial culture indicate that numbers of bacteria per granuloma are variable and generally low, ranging from sterile granulomas to 10^6 bacteria per granuloma (JLF and PLL, in preparation). *M.tb* were often not abundant in granulomas, with most granulomas having either no or very small numbers of visible bacteria per 5 um tissue section. In granulomas where bacteria were visible, bacilli were present in a variety of locations including in epithelioid macrophages (Figure 7A), intermixed with neutrophils at the caseum-macrophage interface (Figure 7A), and in giant cells at the granuloma's periphery (Figure 7B). Bacteria were most commonly present as small groups of individual bacilli associated with necrotic appearing cells at the caseum-macrophage interface. Small numbers of individual bacilli were also occasionally visible deep in the necrotic regions of caseous lesions (Figure 7B). Auramine-rhodamine-stained objects that did not appear to be intact bacteria were also occasionally visible in epithelioid macrophages adjacent to foamy macrophages with elongated morphologies consistent with foamy HAM56+ cells (Figure 7C). Interestingly, fibrotic granulomas from latent disease contained a ring of auramine-rhodamine-stained mycolic acid at the fibroblast-collagen-transformed caseum interface (Figure 7D) suggesting persistence and diffusion of bacterial antigen after most of the bacteria appeared to have been cleared.

Non-necrotic and necrotic granulomas from humans are similar to cynomolgus macaques with respect to macrophage subset, NOS and arginase localization

The organization of macrophage subsets in non-necrotic and necrotic human granulomas was grossly similar to macaque granulomas. In non-necrotic human granulomas (Figure 8A), CD163+ macrophages were present throughout the granuloma, with cells in the outer regions commonly co-expressing HAM56 (Figure 7B). Necrotic granulomas (Figure 8F) had large numbers of CD163+HAM56+ macrophages in the peripheral tissue while cells in the lymphocyte cuff were more likely to be CD163+HAM56- (Figure 8G). While HAM56 staining adjacent to the caseum was observed, it was not as intense or as distinct as it was in macaque granulomas. Epithelioid macrophages in non-necrotic and necrotic granulomas

strongly expressed CD68 (Figure 8D, 8I). Clusters of macrophages in the peripheral tissue surrounding these granulomas were HAM56+CD68+CD163+ (arrows, Figure 8G, 8I) whereas these clusters in macaques were HAM56-CD68+CD163+ (data not shown). Calprotectin-expressing neutrophils were present and their distribution in non-necrotic granulomas was similar to that observed in macaque granulomas (Figure 8B). While we observed neutrophils in necrotic granulomas, they were not as numerous as they were in macaque granulomas and did not appear to accumulate at the macrophage-caseum interface (Figure 8G).

iNOS was expressed at low levels by macrophages distributed throughout human non-necrotic granulomas or adjacent to caseum in necrotic granulomas (Figure 8C, 8H). Unidentified cells expressing high levels of iNOS were present in regions of non-necrotic granulomas and in the lymphocyte cuff of necrotic granulomas. Similarly-stained cells were observed in some macaque granulomas. CD68+ macrophages in human granulomas frequently expressed eNOS (Figure 8D, 8I), and clusters of HAM56+CD68+CD163+ macrophages in the tissue adjacent to granulomas stained particularly strong for eNOS (arrows). Arg1 expression was similar that seen in macaque granulomas: Arg1 staining was visible throughout cellular regions of granulomas with little evidence for region-specific expression and Arg1 expression frequently occurred in cells that also expressed iNOS (Figure 8C, 8H). As has been previously reported (26), there was little Arg2 expressed in human granulomas. Human granulomas contained scattered Arg2-expressing cells but Arg2 staining did not appear to be as tightly correlated with neutrophils as it was in macaque granulomas (Figure 8E, 8J).

Discussion

Large populations of macrophages are a prominent feature of tuberculous granulomas yet there are many unanswered questions surrounding the spatial organization of macrophage subsets in granulomas and whether macrophages have microenvironment-specific homeostatic or bactericidal functions. Much of what we know about granuloma macrophages comes from animal models that may not represent the spectrum of pathology seen in humans or has been derived from cells removed from the context of the granuloma. To address these questions, we used immunohistochemistry to clarify the interplay of microenvironment and macrophage biology by identifying macrophage subsets, and arginase and nitric oxide synthase expression in granulomas from cynomolgus macaques, a nonhuman primate that recapitulates human TB (4). We found that granulomas have macrophage subsets that are stratified into pro- and anti-inflammatory regions with the implication that this organization may limit immunopathogenic antimicrobial activity to bacteria-rich microenvironments by surrounding them with a layer of cells with anti-inflammatory phenotypes.

The importance of NOS in human TB is controversial (37-39). In mice, elimination of nitric oxide leads to higher bacterial numbers and decreased survival time (10, 39). *M.tb* has limited sensitivity to nitric oxide-mediated killing (40-42), and mice with functional iNOS still die from TB, demonstrating that nitrogen radical production alone does not correlate with protection. Humans with TB also express iNOS (13-15), but even though they do not generate NO as vigorously as mice, the human immune system is better at containing *M.tb* and most infections do not progress to active TB. Our data demonstrate that macaque macrophages can express NOS, and granulomas have higher eNOS and iNOS expression than uninfected lung tissue. Epithelioid macrophages can be associated with *M.tb* bacilli in granulomas, and iNOS and eNOS expression, with low levels of Arg1 expression, suggests that nitric oxide production by these cells is an active component of the anti-*M.tb* response in macaques. Fibrocalcific granulomas associated with latent *M.tb* infection also had iNOS-

positive cells, implying that even successful immune responses during latency retain low levels of iNOS expression. This population of iNOS-expressing cells remains in place, presumably, either because stimulus is provided by residual mycobacterial antigens or the low numbers of viable bacilli that may be present in these lesions. The surprising amount of eNOS in granulomas in active disease brings up the question of whether it participates in protection against *M.tb*. Its localization to plasma membranes instead of phagosome-like structures suggests it may not be appropriately positioned to target intracellular bacteria. Alternatively, eNOS produces superoxide when "uncoupled" if tetrahydrobiopterin or L-arginine are limiting (43, 44) or through protein kinase C-ζ–mediated processes following exposure to hypochlorous acid (45). Superoxide in the presence of nitric oxide generates peroxynitrite which is lethal to *M.tb*(46). There remains much to be learned about epithelioid macrophage biology in situ, and eNOS expression may serve alternative functions that are not directly bactericidal but still contribute to protection. However, nitric oxide may also downregulate immune responses in the granuloma, for example by inhibiting T cell functions as has been demonstrated in other experimental systems (21, 47-49) or by limiting inflammasome activation and subsequent IL-1β secretion (50).

Arginases can compete with NOS for L-arginine thereby downregulating NO production and generating L-ornithine, an amino acid that can be used for proline synthesis (19), which is utilized for synthesis of proline-rich proteins such as collagen in granulomas, wound healing and fibrotic tissues, or for polyamine synthesis (19). In mice, Arg1 expression occurs in M2-polarized (anti-inflammatory) macrophages (17, 51, 52) and in wound healing macrophages (53). It has been demonstrated that conversion of arginine to proline in anti-inflammatory macrophages is dependent on Arg1 (54), consistent with the notion that arginase-derived ornithine may promote synthesis of collagen (leading to fibrosis) in tuberculous granulomas. However, ablation of macrophage Arg1 expression resulted in increased fibrosis in mice infected with *Schistosoma mansoni* (21), indicating that fibrosis may not be enhanced by Arg1 in all circumstances. Arginase expression is correlated with decreased protection against acute *M.tb* infection in mice (24, 25), likely reflecting depletion of L-arginine substrate for nitric oxide synthesis. Protective immune responses against *M.tb* may require both pro-inflammatory macrophages with bactericidal activity and pro-healing anti-inflammatory macrophages to limit immunopathology. Moreover, primate granulomas are highly organized and protection would be contingent upon appropriate spatial expression of NOS and arginase expression. Because of this, we hypothesized $Arg1^{-}NOS^{+}$ macrophages would be present in bacilli-rich microenvironments and $Arg1^{+}NOS^{-}$ macrophages along the outer margins. Instead, we found substantial co-expression of NOS and arginase throughout necrotic granulomas, and elevated Arg1 expression in the lymphocyte cuff region, indicating the ratio of NOS:arginase expression is most likely to be a factor determining functional macrophage polarity in primates. The paucity of Arg1 expression in epithelioid macrophages also suggests that competition for L-arginine by Arg1 may be a critical posttranscriptional determinant of macrophage polarity and NOS activity in primate tuberculous granulomas. The abundance of L-arginine-utilizing enzymes in granulomas may also lead to L-arginine depletion. Consequences of this depletion on T cell function may include downregulation of T cell TCR-ζ expression (47, 48), activation (48, 49), proliferation (48, 49) and cytokine secretion (21, 48). Thus arginase and NOS expression may decrease proinflammatory T cell responses and modulate macrophage function.

Macrophage diversity and spatial organization of cells within granulomas are significant yet underappreciated aspects of the biology of TB. Alveolar macrophages in cynomolgus macaques are predominately $CD11c^{+}CD68^{+}CD163^{+}$ but macrophage phenotypes in the granuloma are considerably more complex. CD163 expression delineated two macrophage subsets: $CD11c^{+}CD68^{+}CD163^{+}$ / $CD68^{-}CD163^{+}$ cells and $CD68^{+}CD163^{dim}$ / $CD68^{+}CD163^{-}$ cells. CD163 expression has been identified as a marker of alternative

activation (M2) (52, 55), and the abundance of these cells in outer regions of granulomas are phosphor-STAT3 positive (data not shown), an indicator of IL-10 signaling in alternatively activated macrophages (56, 57), and have a lower ratio of iNOS:Arg1 expression relative to epithelioid macrophages suggests these cells may not be actively bactericidal. In contrast, $CD11c^{+}CD68^{+}CD163^{-}$ epithelioid macrophages are present in regions with the largest number of bacteria or bacterial antigens and had classically-activated NOS-expressing phenotypes. HAM56, a reported marker for foamy macrophages (58-60), was also associated with cells at the epithelioid macrophage-caseum interface, a position similar to the location of Oil Red O-stained macrophages in human granulomas (2, 61). In addition to acting as mediators of L-arginine metabolism in granulomas, granuloma macrophages may be important sources of pro-inflammatory and anti-inflammatory cytokine production that may also influence how successful a granuloma is at containing bacterial replication and dissemination.

The epithelioid macrophage-caseum interface also contained significant numbers of neutrophils. The role of neutrophils in TB is controversial (62). Murine TB models indicate neutrophil infiltration is enabled by impaired adaptive immune responses and leads to increased pathology and accelerated disease progression (63), and a neutrophil transcriptional signature in human blood differentiated persons with active TB or latent infection (64). Similarly, granulomas from cynomolgus macaques with poorly controlled TB can contain large numbers of neutrophils (5), oftentimes in close proximity to bacilli. *M.tb* is resistant to neutrophil-mediated killing (62, 65) and neutrophils in the airways of TB patients commonly contain replicating *M.tb*(66). Moreover, neutrophil cytosol is rich in calprotectin, an antimicrobial peptide that is supportive of *M.tb* growth in vitro (67) further suggesting they are not restricting *M.tb* survival and replication. Moreover, the proximity of degenerating neutrophils with bacilli suggests it is also positive that these cells may provide a nutrient source for *M.tb*. Neutrophils in granulomas can express iNOS and stain positively for nitrotyrosine, demonstrating that they generate NO but it is unknown whether this influences bacterial containment. In addition to commonly-considered neutrophil effector mechanisms, neutrophils can express cytokines including TNF, IL-1β, IL-12 and VEGF (68, 69) and participate in cross-priming of CD8+ T cells (70), suggesting neutrophils may exert unappreciated and unknown effects on protection.

These data on macrophage phenotypes, neutrophil distribution and immune function present a dynamic granuloma-scale picture of immune function in human and primate granulomas. Active lesions display a gradient of anti- and pro-inflammatory phenotypes, with anti-inflammatory $CD163^{+}iNOS^{+}Arg1^{high}$ macrophages on outer margins and pro-inflammatory $CD11C^{+}CD68^{+}CD163^{dim}iNOS^{+}eNOS^{+}Arg1^{low}$ macrophages toward the center, thus making it possible to mount antibacterial responses safely away from uninvolved tissue. Fibrocalcific granulomas retain aspects of this gradient, but the macrophage populations are biased toward anti-inflammatory phenotypes ($CD68^{-}CD163^{+}$), possibly due to lower numbers of bacilli in these granulomas (71). iNOS expression still occurs in these granulomas, suggesting some continued presence of anti-mycobacterial activity is required for controlling any bacteria remaining in these lesions. The concept of a cell and effector gradient is also supported by mathematical modeling (29). A better understanding of what constitutes a protective macrophage phenotype in a particular microenvironment, and techniques to promote specific macrophage phenotypes may provide important avenues for immunotherapeutic treatment of TB.

Supplementary Material

Refer to Web version on PubMed Central for supplementary material.

Acknowledgments

The authors thank Jennifer Linderman and Nicholas Clifone for their critical reading of the manuscript and helpful discussions. We also thank the patients and staff of National Masan Tuberculosis Hospital for their time and participation in our studies. We are grateful to the Flynn lab for helpful discussions and the excellent veterinary staff.

Financial support by: Support for this study was provided by NIH grants HL074845 (JLF), HL106804 (JLF and DEK), HL092883 (JLF and DEK), EB012579 (DEK and JLF), GM057384-11 (SMM), Division of Intramural Research, NIAID, NIH and the Korean Ministry of Health, Welfare and Family Affairs (CEB), AI060525-05 (JLF, supporting JTM), AI077183 (JTM), the Bill and Melinda Gates Foundation (JLF, PLL, CEB), NIH K08 AI063101 (PLL) Otis Foundation (PLL) and the Heiser Program for Research in Tuberculosis and Leprosy (JTM).

References

1. Lawn SD, Zumla AI. Tuberculosis. Lancet. 2011; 378:57–72. [PubMed: 21420161]
2. Russell DG, Cardona PJ, Kim MJ, Allain S, Altare F. Foamy macrophages and the progression of the human tuberculosis granuloma. Nat Immunol. 2009; 10:943–948. [PubMed: 19692995]
3. Flynn, JL.; Klein, E., editors. Pulmonary Tuberculosis in Monkeys. CRC Press, Talor & Francis Publishers; 2010.
4. Capuano SV 3rd, Croix DA, Pawar S, Zinovik A, Myers A, Lin PL, Bissel S, Fuhrman C, Klein E, Flynn JL. Experimental Mycobacterium tuberculosis infection of cynomolgus macaques closely resembles the various manifestations of human M tuberculosis infection. Infect Immun. 2003; 71:5831–5844. [PubMed: 14500505]
5. Lin PL, Rodgers M, Smith L, Bigbee M, Myers A, Bigbee C, Chiosea I, Capuano SV, Fuhrman C, Klein E, Flynn JL. Quantitative comparison of active and latent tuberculosis in the cynomolgus macaque model. Infect Immun. 2009; 77:4631–4642. [PubMed: 19620341]
6. Lin PL, Rodgers M, Smith L, Bigbee M, Myers A, Bigbee C, Chiosea I, Capuano SV, Fuhrman C, Klein E, Flynn J. Quantitative comparison of active and latent tuberculosis in the cynomolgus macaque model. Infect Immun. 2009
7. Leong, F.; Seokyong, E.; Laura, V.; Clifton, B. A Color Atlas of Comparative Pathology of Pulmonary Tuberculosis. CRC Press; 2010. Pathology of Tuberculosis in the Human Lung; p. 53-81.
8. Marino S, Linderman JJ, Kirschner DE. A multifaceted approach to modeling the immune response in tuberculosis. Wiley Interdiscip Rev Syst Biol Med. 2011; 3:479–489. [PubMed: 21197656]
9. Ray JC, Flynn JL, Kirschner DE. Synergy between individual TNF-dependent functions determines granuloma performance for controlling Mycobacterium tuberculosis infection. J Immunol. 2009; 182:3706–3717. [PubMed: 19265149]
10. Adams LB, Dinauer MC, Morgenstern DE, Krahenbuhl JL. Comparison of the roles of reactive oxygen and nitrogen intermediates in the host response to Mycobacterium tuberculosis using transgenic mice. Tuber Lung Dis. 1997; 78:237–246. [PubMed: 10209678]
11. MacMicking JD, North RJ, LaCourse R, Mudgett JS, Shah SK, Nathan CF. Identification of nitric oxide synthase as a protective locus against tuberculosis. Proc Natl Acad Sci U S A. 1997; 94:5243–5248. [PubMed: 9144222]
12. Scanga CA, Mohan VP, Tanaka K, Alland D, Flynn JL, Chan J. The inducible nitric oxide synthase locus confers protection against aerogenic challenge of both clinical and laboratory strains of Mycobacterium tuberculosis in mice. Infect Immun. 2001; 69:7711–7717. [PubMed: 11705952]
13. Choi HS, Rai PR, Chu HW, Cool C, Chan ED. Analysis of nitric oxide synthase and nitrotyrosine expression in human pulmonary tuberculosis. Am J Respir Crit Care Med. 2002; 166:178–186. [PubMed: 12119230]
14. Schon T, Elmberger G, Negesse Y, Pando RH, Sundqvist T, Britton S. Local production of nitric oxide in patients with tuberculosis. Int J Tuberc Lung Dis. 2004; 8:1134–1137. [PubMed: 15455601]
15. Nicholson S, Bonecini-Almeida Mda G, Lapa e Silva JR, Nathan C, Xie QW, Mumford R, Weidner JR, Calaycay J, Geng J, Boechat N, Linhares C, Rom W, Ho JL. Inducible nitric oxide

synthase in pulmonary alveolar macrophages from patients with tuberculosis. J Exp Med. 1996; 183:2293–2302. [PubMed: 8642338]

16. Nathan C, Shiloh MU. Reactive oxygen and nitrogen intermediates in the relationship between mammalian hosts and microbial pathogens. Proc Natl Acad Sci U S A. 2000; 97:8841–8848. [PubMed: 10922044]
17. Gordon S, Martinez FO. Alternative activation of macrophages: mechanism and functions. Immunity. 2010; 32:593–604. [PubMed: 20510870]
18. Byers DE, Holtzman MJ. Alternatively activated macrophages and airway disease. Chest. 2011; 140:768–774. [PubMed: 21896520]
19. Morris SM Jr. Arginine metabolism: boundaries of our knowledge. J Nutr. 2007; 137:1602S–1609S. [PubMed: 17513435]
20. Shearer JD, Richards JR, Mills CD, Caldwell MD. Differential regulation of macrophage arginine metabolism: a proposed role in wound healing. Am J Physiol. 1997; 272:E181–190. [PubMed: 9124321]
21. Pesce JT, Ramalingam TR, Mentink-Kane MM, Wilson MS, El Kasmi KC, Smith AM, Thompson RW, Cheever AW, Murray PJ, Wynn TA. Arginase-1-expressing macrophages suppress Th2 cytokine-driven inflammation and fibrosis. PLoS Pathog. 2009; 5:e1000371. [PubMed: 19360123]
22. Pegg AE. Mammalian polyamine metabolism and function. IUBMB Life. 2009; 61:880–894. [PubMed: 19603518]
23. Barron L, Wynn TA. Macrophage activation governs schistosomiasis-induced inflammation and fibrosis. Eur J Immunol. 2011; 41:2509–2514. [PubMed: 21952807]
24. El Kasmi KC, Qualls JE, Pesce JT, Smith AM, Thompson RW, Henao-Tamayo M, Basaraba RJ, Konig T, Schleicher U, Koo MS, Kaplan G, Fitzgerald KA, Tuomanen EI, Orme IM, Kanneganti TD, Bogdan C, Wynn TA, Murray PJ. Toll-like receptor-induced arginase 1 in macrophages thwarts effective immunity against intracellular pathogens. Nat Immunol. 2008; 9:1399–1406. [PubMed: 18978793]
25. Schreiber T, Ehlers S, Heitmann L, Rausch A, Mages J, Murray PJ, Lang R, Holscher C. Autocrine IL-10 induces hallmarks of alternative activation in macrophages and suppresses antituberculosis effector mechanisms without compromising T cell immunity. J Immunol. 2009; 183:1301–1312. [PubMed: 19561100]
26. Pessanha AP, Martins RA, Mattos-Guaraldi AL, Vianna A, Moreira LO. Arginase-1 expression in granulomas of tuberculosis patients. FEMS Immunol Med Microbiol. 2012
27. Zea AH, Culotta KS, Ali J, Mason C, Park HJ, Zabaleta J, Garcia LF, Ochoa AC. Decreased expression of CD3zeta and nuclear transcription factor kappa B in patients with pulmonary tuberculosis: potential mechanisms and reversibility with treatment. J Infect Dis. 2006; 194:1385–1393. [PubMed: 17054067]
28. Mosser DM. The many faces of macrophage activation. J Leukoc Biol. 2003; 73:209–212. [PubMed: 12554797]
29. Fallahi-Sichani M, Schaller MA, Kirschner DE, Kunkel SL, Linderman JJ. Identification of key processes that control tumor necrosis factor availability in a tuberculosis granuloma. PLoS Comput Biol. 2010; 6:e1000778. [PubMed: 20463877]
30. Kepka-Lenhart D, Ash DE, Morris SM. Determination of mammalian arginase activity. Methods Enzymol. 2008; 440:221–230. [PubMed: 18423220]
31. Livak KJ, Schmittgen TD. Analysis of relative gene expression data using real-time quantitative PCR and the 2(-Delta Delta C(T)) Method. Methods. 2001; 25:402–408. [PubMed: 11846609]
32. Pawar SN, Mattila JT, Sturgeon TJ, Lin PL, Narayan O, Montelaro RC, Flynn JL. Comparison of the effects of pathogenic simian human immunodeficiency virus strains SHIV-89.6P and SHIV-KU2 in cynomolgus macaques. AIDS Res Hum Retroviruses. 2008; 24:643–654. [PubMed: 18366326]
33. El-Zammar OA, Katzenstein AL. Pathological diagnosis of granulomatous lung disease: a review. Histopathology. 2007; 50:289–310. [PubMed: 17257125]
34. Jones, TC.; Hunt, RD.; King, NW. Veterinary pathology. Williams & Wilkins; Baltimore, Md: 1997.

35. Turk JL, Narayanan RB. The origin, morphology, and function of epithelioid cells. Immunobiology. 1982; 161:274–282. [PubMed: 7047374]
36. Hamann J, Koning N, Pouwels W, Ulfman LH, van Eijk M, Stacey M, Lin HH, Gordon S, Kwakkenbos MJ. EMR1, the human homolog of F4/80, is an eosinophil-specific receptor. Eur J Immunol. 2007; 37:2797–2802. [PubMed: 17823986]
37. Chan ED, Chan J, Schluger NW. What is the role of nitric oxide in murine and human host defense against tuberculosis?Current knowledge. Am J Respir Cell Mol Biol. 2001; 25:606–612. [PubMed: 11713103]
38. Nathan C. Role of iNOS in human host defense. Science. 2006; 312:1874–1875. author reply 1874-1875. [PubMed: 16809512]
39. Nathan C. Inducible nitric oxide synthase in the tuberculous human lung. Am J Respir Crit Care Med. 2002; 166:130–131. [PubMed: 12119220]
40. Lee WL, Gold B, Darby C, Brot N, Jiang X, de Carvalho LP, Wellner D, St John G, Jacobs WR Jr, Nathan C. Mycobacterium tuberculosis expresses methionine sulphoxide reductases A and B that protect from killing by nitrite and hypochlorite. Mol Microbiol. 2009; 71:583–593. [PubMed: 19040639]
41. Ohno H, Zhu G, Mohan VP, Chu D, Kohno S, Jacobs WR Jr, Chan J. The effects of reactive nitrogen intermediates on gene expression in Mycobacterium tuberculosis. Cell Microbiol. 2003; 5:637–648. [PubMed: 12925133]
42. Darwin KH, Ehrt S, Gutierrez-Ramos JC, Weich N, Nathan CF. The proteasome of Mycobacterium tuberculosis is required for resistance to nitric oxide. Science. 2003; 302:1963–1966. [PubMed: 14671303]
43. Werner ER, Gorren AC, Heller R, Werner-Felmayer G, Mayer B. Tetrahydrobiopterin and nitric oxide: mechanistic and pharmacological aspects. Exp Biol Med (Maywood). 2003; 228:1291–1302. [PubMed: 14681545]
44. Alp NJ, Channon KM. Regulation of endothelial nitric oxide synthase by tetrahydrobiopterin in vascular disease. Arterioscler Thromb Vasc Biol. 2004; 24:413–420. [PubMed: 14656731]
45. Xu J, Xie Z, Reece R, Pimental D, Zou MH. Uncoupling of endothelial nitric oxidase synthase by hypochlorous acid: role of NAD(P)H oxidase-derived superoxide and peroxynitrite. Arterioscler Thromb Vasc Biol. 2006; 26:2688–2695. [PubMed: 17023679]
46. Yu K, Mitchell C, Xing Y, Magliozzo RS, Bloom BR, Chan J. Toxicity of nitrogen oxides and related oxidants on mycobacteria: M tuberculosis is resistant to peroxynitrite anion. Tuber Lung Dis. 1999; 79:191–198. [PubMed: 10692986]
47. Rodriguez PC, Zea AH, DeSalvo J, Culotta KS, Zabaleta J, Quiceno DG, Ochoa JB, Ochoa AC. L-arginine consumption by macrophages modulates the expression of CD3 zeta chain in T lymphocytes. J Immunol. 2003; 171:1232–1239. [PubMed: 12874210]
48. Zea AH, Rodriguez PC, Culotta KS, Hernandez CP, DeSalvo J, Ochoa JB, Park HJ, Zabaleta J, Ochoa AC. L-Arginine modulates CD3zeta expression and T cell function in activated human T lymphocytes. Cell Immunol. 2004; 232:21–31. [PubMed: 15922712]
49. Choi BS, Martinez-Falero IC, Corset C, Munder M, Modolell M, Muller I, Kropf P. Differential impact of L-arginine deprivation on the activation and effector functions of T cells and macrophages. J Leukoc Biol. 2009; 85:268–277. [PubMed: 19008294]
50. Mishra BB, Rathinam VA, Martens GW, Martinot AJ, Kornfeld H, Fitzgerald KA, Sassetti CM. Nitric oxide controls the immunopathology of tuberculosis by inhibiting NLRP3 inflammasome-dependent processing of IL-1beta. Nat Immunol. 2013; 14:52–60. [PubMed: 23160153]
51. Biswas SK, Mantovani A. Macrophage plasticity and interaction with lymphocyte subsets: cancer as a paradigm. Nat Immunol. 2010; 11:889–896. [PubMed: 20856220]
52. Cassol E, Cassetta L, Alfano M, Poli G. Macrophage polarization and HIV-1 infection. J Leukoc Biol. 2010; 87:599–608. [PubMed: 20042468]
53. Daley JM, Brancato SK, Thomay AA, Reichner JS, Albina JE. The phenotype of murine wound macrophages. J Leukoc Biol. 2010; 87:59–67. [PubMed: 20052800]
54. Hesse M, Modolell M, La Flamme AC, Schito M, Fuentes JM, Cheever AW, Pearce EJ, Wynn TA. Differential regulation of nitric oxide synthase-2 and arginase-1 by type 1/type 2 cytokines in vivo:

granulomatous pathology is shaped by the pattern of L-arginine metabolism. J Immunol. 2001; 167:6533–6544. [PubMed: 11714822]

55. Niino D, Komohara Y, Murayama T, Aoki R, Kimura Y, Hashikawa K, Kiyasu J, Takeuchi M, Suefuji N, Sugita Y, Takeya M, Ohshima K. Ratio of M2 macrophage expression is closely associated with poor prognosis for Angioimmunoblastic T-cell lymphoma (AITL). Pathol Int. 2010; 60:278–283. [PubMed: 20403029]
56. Stumpo R, Kauer M, Martin S, Kolb H. Alternative activation of macrophage by IL-10. Pathobiology. 1999; 67:245–248. [PubMed: 10725794]
57. Niemand C, Nimmesgern A, Haan S, Fischer P, Schaper F, Rossaint R, Heinrich PC, Muller-Newen G. Activation of STAT3 by IL-6 and IL-10 in primary human macrophages is differentially modulated by suppressor of cytokine signaling 3. J Immunol. 2003; 170:3263–3272. [PubMed: 12626585]
58. Ihling C, Gobel HR, Lippoldt A, Wessels S, Paul M, Schaefer HE, Zeiher AM. Endothelin-1-like immunoreactivity in human atherosclerotic coronary tissue: a detailed analysis of the cellular distribution of endothelin-1. J Pathol. 1996; 179:303–308. [PubMed: 8774487]
59. Cummings TJ, Hulette CM, Bigner SH, Riggins GJ, McLendon RE. Ham56-immunoreactive macrophages in untreated infiltrating gliomas. Arch Pathol Lab Med. 2001; 125:637–641. [PubMed: 11300934]
60. Oleszak EL, Zaczynska E, Bhattacharjee M, Butunoi C, Legido A, Katsetos CD. Inducible nitric oxide synthase and nitrotyrosine are found in monocytes/macrophages and/or astrocytes in acute, but not in chronic, multiple sclerosis. Clin Diagn Lab Immunol. 1998; 5:438–445. [PubMed: 9665945]
61. Peyron P, Vaubourgeix J, Poquet Y, Levillain F, Botanch C, Bardou F, Daffe M, Emile JF, Marchou B, Cardona PJ, de Chastellier C, Altare F. Foamy macrophages from tuberculous patients' granulomas constitute a nutrient-rich reservoir for M. tuberculosis persistence. PLoS Pathog. 2008; 4:e1000204. [PubMed: 19002241]
62. Lowe DM, Redford PS, Wilkinson RJ, O'Garra A, Martineau AR. Neutrophils in tuberculosis: friend or foe? Trends Immunol. 2012; 33:14–25. [PubMed: 22094048]
63. Nandi B, Behar SM. Regulation of neutrophils by interferon-gamma limits lung inflammation during tuberculosis infection. J Exp Med. 2011; 208:2251–2262. [PubMed: 21967766]
64. Berry MP, Graham CM, McNab FW, Xu Z, Bloch SA, Oni T, Wilkinson KA, Banchereau R, Skinner J, Wilkinson RJ, Quinn C, Blankenship D, Dhawan R, Cush JJ, Mejias A, Ramilo O, Kon OM, Pascual V, Banchereau J, Chaussabel D, O'Garra A. An interferon-inducible neutrophil-driven blood transcriptional signature in human tuberculosis. Nature. 2010; 466:973–977. [PubMed: 20725040]
65. Corleis B, Korbel D, Wilson R, Bylund J, Chee R, Schaible UE. Escape of Mycobacterium tuberculosis from Oxidative Killing by Neutrophils. Cell Microbiol. 2012
66. Eum SY, Kong JH, Hong MS, Lee YJ, Kim JH, Hwang SH, Cho SN, Via LE, Barry CE 3rd. Neutrophils are the predominant infected phagocytic cells in the airways of patients with active pulmonary TB. Chest. 2010; 137:122–128. [PubMed: 19749004]
67. Pechkovsky DV, Zalutskaya OM, Ivanov GI, Misuno NI. Calprotectin (MRP8/14 protein complex) release during mycobacterial infection in vitro and in vivo. FEMS Immunol Med Microbiol. 2000; 29:27–33. [PubMed: 10967257]
68. Scapini P, Lapinet-Vera JA, Gasperini S, Calzetti F, Bazzoni F, Cassatella MA. The neutrophil as a cellular source of chemokines. Immunol Rev. 2000; 177:195–203. [PubMed: 11138776]
69. Kasama T, Miwa Y, Isozaki T, Odai T, Adachi M, Kunkel SL. Neutrophil-derived cytokines: potential therapeutic targets in inflammation. Curr Drug Targets Inflamm Allergy. 2005; 4:273–279. [PubMed: 16101533]
70. Tvinnereim AR, Hamilton SE, Harty JT. Neutrophil involvement in cross-priming CD8+ T cell responses to bacterial antigens. J Immunol. 2004; 173:1994–2002. [PubMed: 15265934]
71. Lin PL, Dartois V, Johnston PJ, Janssen C, Via L, Goodwin MB, Klein E, Barry CE 3rd, Flynn JL. Metronidazole prevents reactivation of latent Mycobacterium tuberculosis infection in macaques. Proc Natl Acad Sci U S A. 2012; 109:14188–14193. [PubMed: 22826237]

Figure 1.

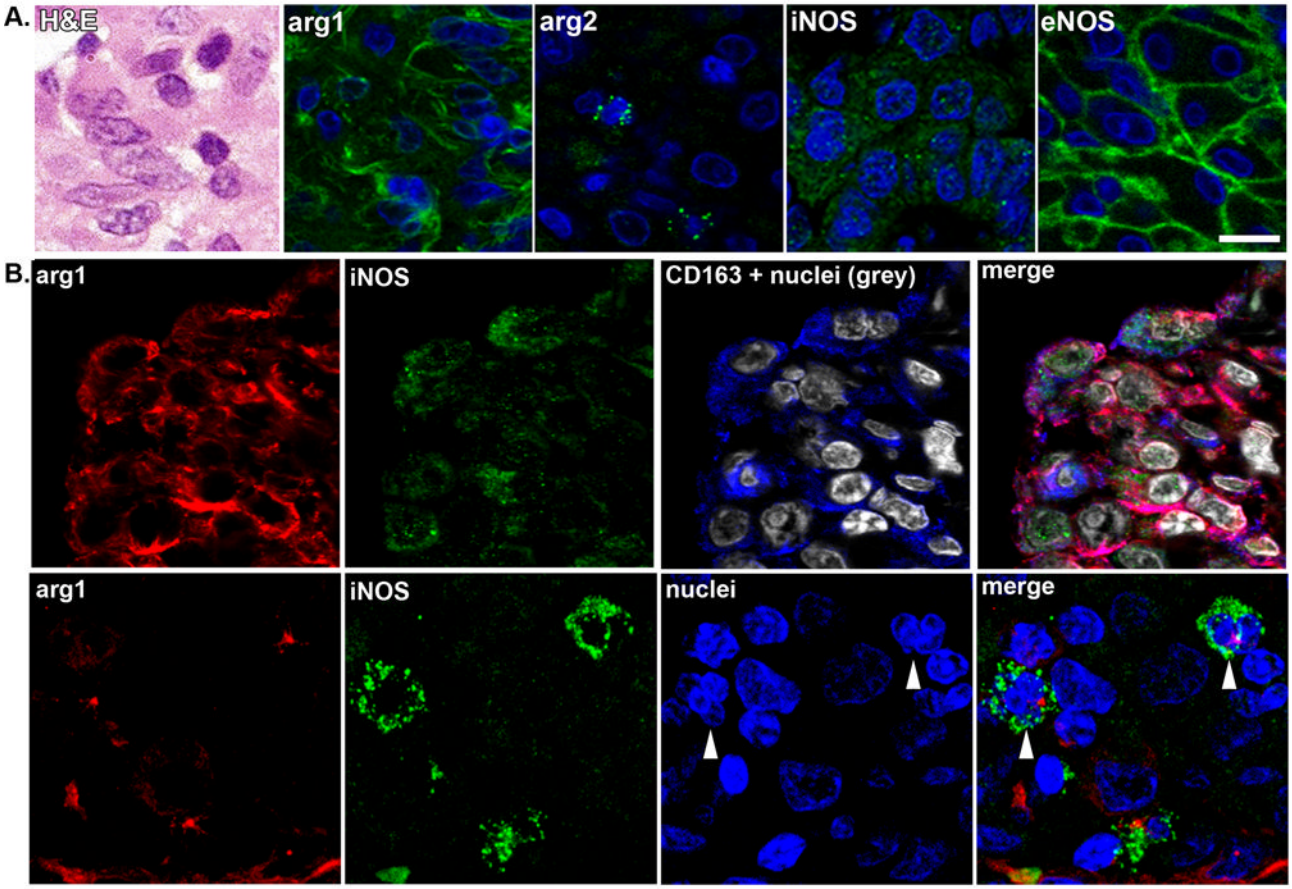

Figure 1. Immunohistochemical identification of arginase and NOS isoforms in cells from cynomolgus macaque granulomas

A. Epithelioid macrophages, as depicted by hematoxylin and eosin staining (H&E) were stained for Arg1, Arg2, iNOS and eNOS (green) and nuclei (blue) and imaged at 600x magnification to represent the unique staining patterns associated with each enzyme. Each panel presents an independent set of epithelioid macrophages in the macrophage region, scale bar represents 20 μm. B. Co-expression of Arg1 (red) and iNOS (green) in CD163+ macrophages (blue, top panel) and in cells with segmented neutrophil-like nuclei (arrowheads, bottom panel). Image acquired at 600x magnification, scale bar represents 20 μm.

Figure 2.

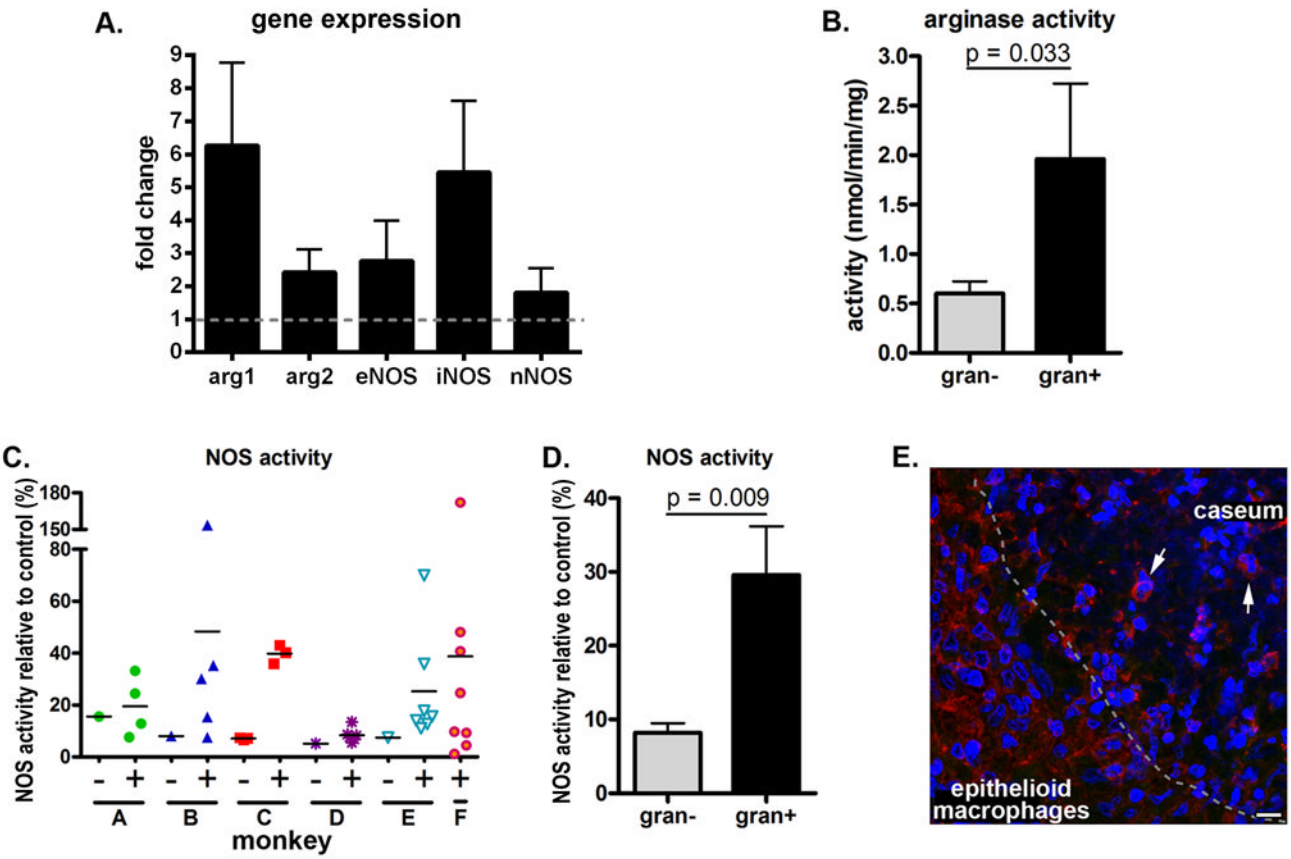

Figure 2. Granulomas contain higher levels of arginase and NOS activity and gene expression than uninvolved lung tissue

Arginase and NOS enzyme activity is from independent experiments using tissues from different animals. A. Relative transcript quantification where granuloma-containing tissues (n=8) are compared against relative transcript abundance in uninvolved tissues (n=4) from four animals. Data represent the mean ± SEM. B. Arginase activity was measured from four uninvolved tissues and six granulomas from five monkeys. Statistical comparison by the Mann-Whitney test. C. NOS activity was measured from seven uninvolved tissues (−) and 35 granulomas (+) from seven animals (A – m23210, B – m21410, C – m22210, D – m5210, E – m22510, F – m22910) showing a trend where involved tissues have more functional enzyme than uninvolved tissue. D. Aggregated data from Figure 2C indicating granulomas have significantly higher mean NOS activity than uninvolved tissues. Statistical comparison by the Mann-Whitney test. E. Immunohistochemical staining of a necrotic granuloma showing strong nitrotyrosine staining at the epithelioid macrophage – caseum interface (indicated by a dashed line) with significant numbers of macrophages and some cells having segmented neutrophil-like nuclei (arrows) that stain positively for nitrotyrosine (red). Scale bar represents 10 μm.

Figure 3.

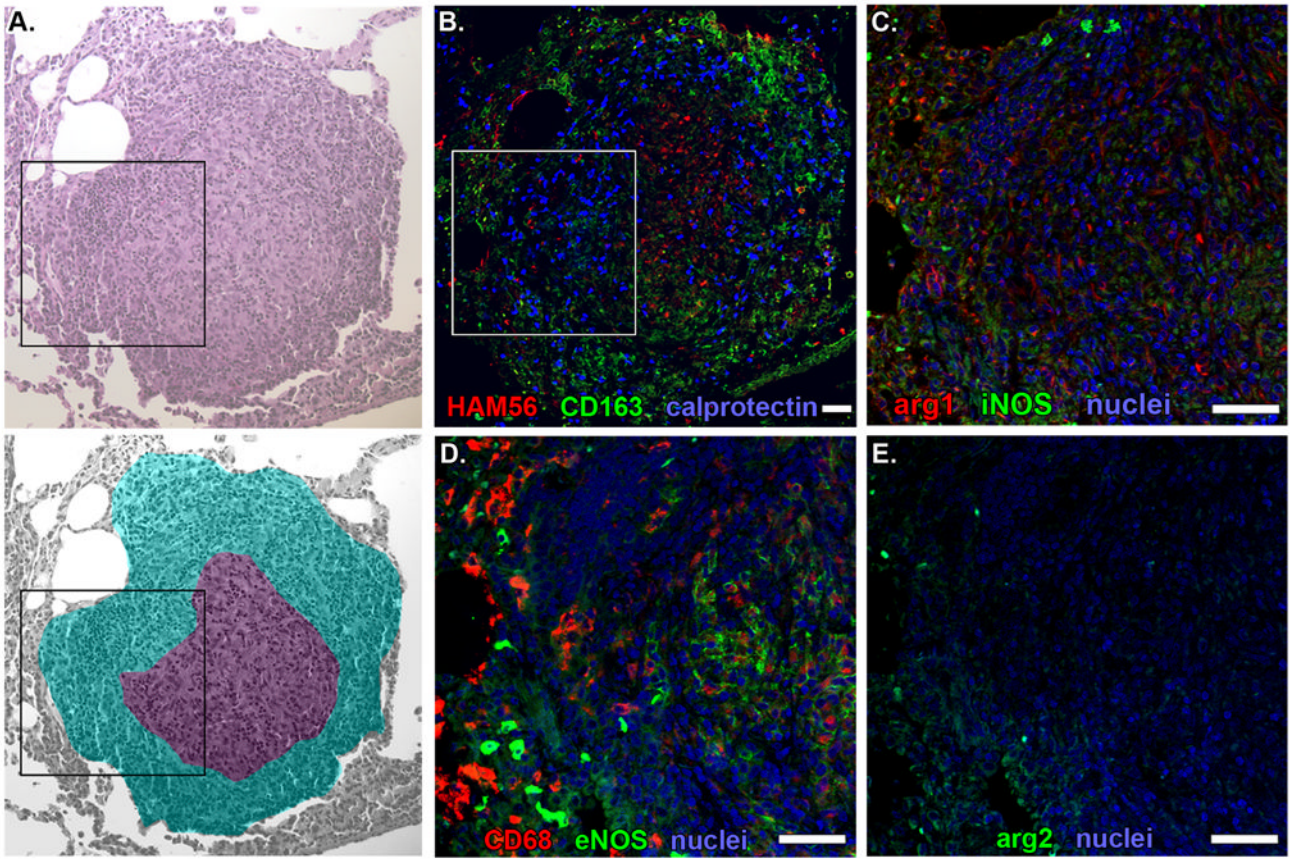

Figure. 3. Macrophage phenotypes and distribution in non-necrotic granulomas from macaques with active TB

Individual panels show serial 5-μm thick sections of a representative non-necrotic granuloma. A. Hematolylin and eosin staining (top) with a pseudocolored representation (bottom) indicating lymphocyte-rich (cyan) and epithelioid macrophage-rich (purple) regions. Black box indicates the region depicted at higher magnification in images C-E. B. Macrophage-specific stains including HAM56 (red), CD163 (green) and calprotectin-stained neutrophils (blue). White box indicates the region depicted at higher magnification in images C-E. C. iNOS (green) and Arg1 (red) expression with nuclei (blue). D. CD68 (red) and eNOS (green) expression with nuclei (blue). E. Arg2 (green) expression with nuclei (blue). Scale bars represent 100 μm.

Figure 4.

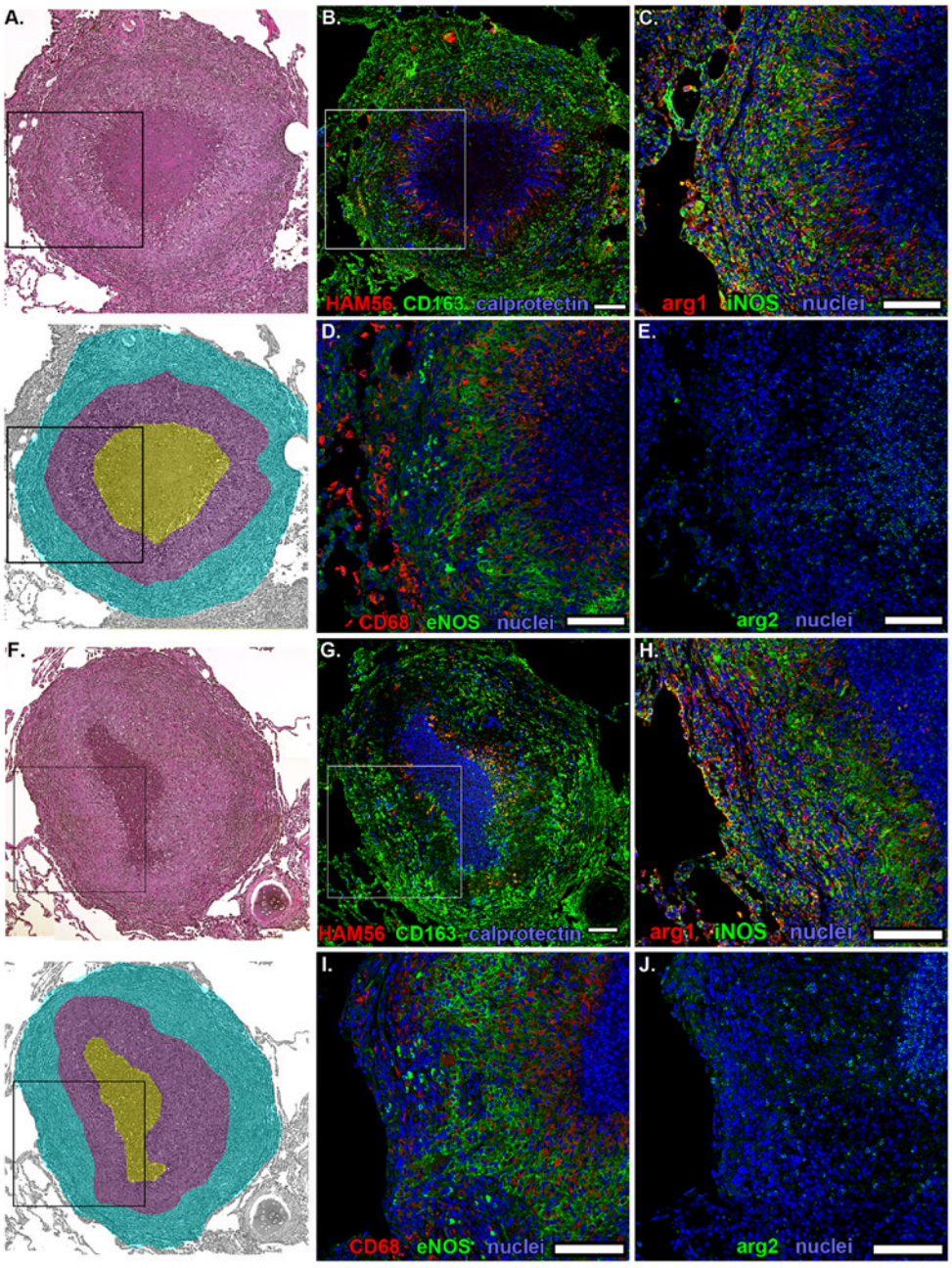

Figure. 4. Macrophage phenotypes and distribution in necrotic and suppurative granulomas from macaques with active TB

Individual panels show serial 5-μm thick sections of representative necrotic and suppurative granulomas. Hematoxylin and eosin staining (top) of a necrotic (A) and suppurative (F) granulomas with pseudocolored representation (bottom) indicating lymphocyte-rich (cyan), epithelioid macrophage-rich (purple) and necrotic (yellow, panel A) or suppurative (yellow, panel F) regions. Black boxes indicate the regions depicted at higher magnification in images C-E and G-J. B, G. Macrophage-specific stains including HAM56 (red), CD163 (green) and calprotectin-stained neutrophils (blue). White box indicates the region depicted at higher magnification in images C-E. C, H. iNOS (green) and Arg1 (red) expression with

nuclei (blue). D, I. CD68 (red) and eNOS (green) expression with nuclei (blue). E, J. Arg2 (green) expression with nuclei (blue). Scale bars represent 100 μm.

Figure 5.

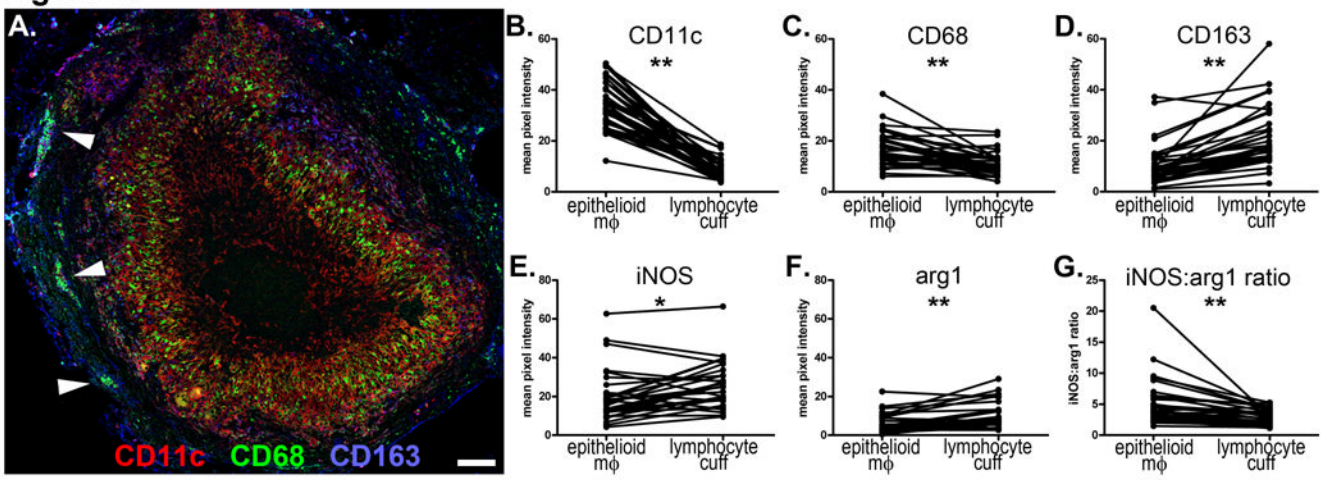

Figure 5. Region-specific expression of macrophage markers, iNOS and Arg1 in necrotic granulomas

A. A necrotic granuloma stained for CD11c (red), CD68 (green) and CD163 (blue) showing distinct stratification of cell populations. Arrowheads indicate clusters of CD11c +CD68+CD163+ alveolar macrophage-like cells. 100x magnification, scale bar represents 100 μm. B-G. Image analysis of necrotic granulomas comparing fluorescence signal intensity of epithelioid macrophage and lymphocyte cuff regions in necrotic granulomas from 4 monkeys (panels B-D: n=37 fields from 18 granulomas, panels E-G: n=30 fields from 18 granulomas). The fields imaged for panels B-D are different from panels E-G but come from granulomas in the same tissue section. B. CD11c. C. CD68. D. CD163. E. iNOS. F. Arg1. G. ratio of iNOS:Arg1 signal intensity showing decreased Arg1 expression in epithelioid macrophage region relative to the lymphocyte cuff. Pairwise comparisons by the Wilcoxon matched-pairs signed rank test;* $p=0.062$, ** $p<0.0001$.

Figure 6.

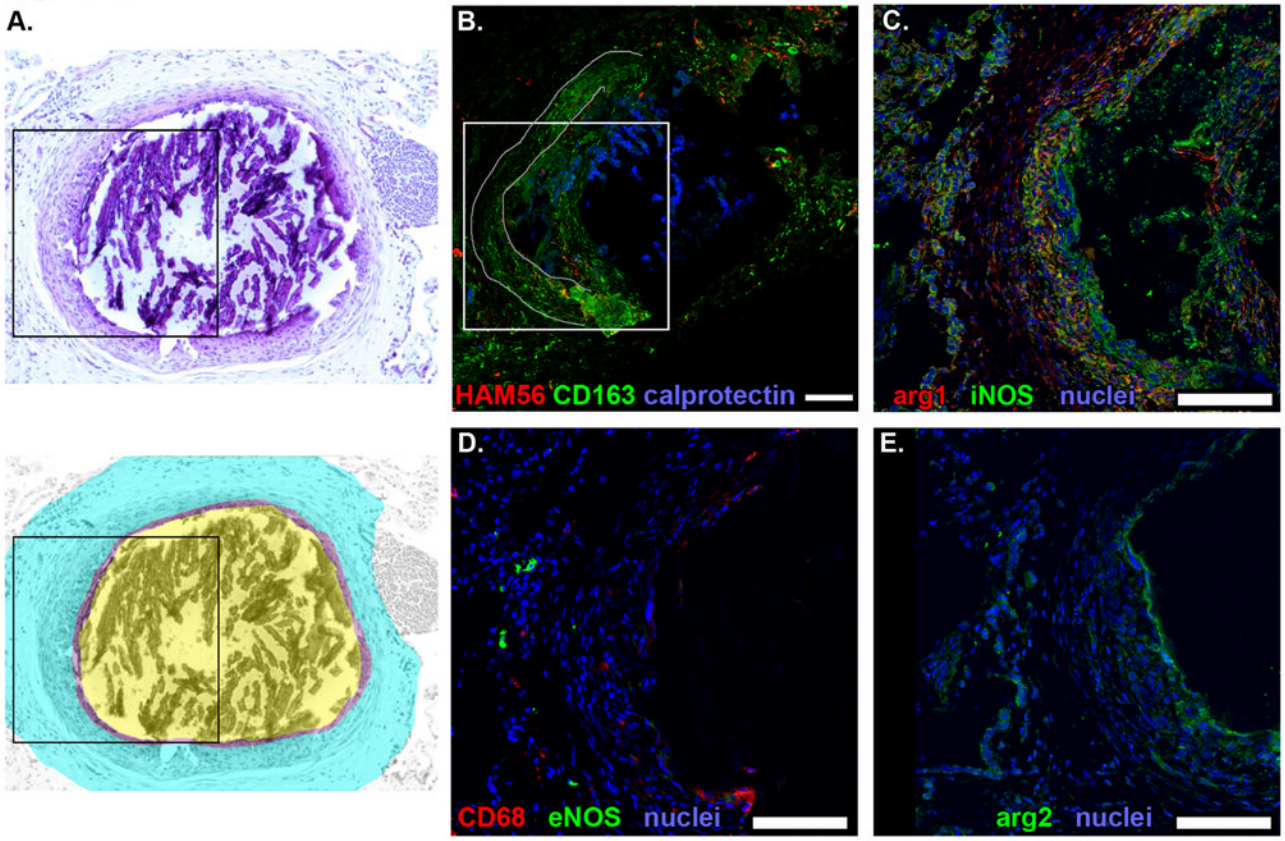

Figure. 6. Macrophage phenotypes and distribution in fibrocalcific granulomas from macaques with latent TB

Individual panels show serial 5-μm thick sections of a representative necrotic granuloma. A. Hematoxylin and eosin (top) with pseudocolored representation (bottom) indicating the outer fibrotic region (cyan), fibro-calcific interface (purple) and central region containing mineralized material (yellow) that shattered during cutting. Dashed line indicates portion of the fibrocalcific interface that is separated from the rest of the granuloma and is present as an artifact in A. Black box indicates the region depicted at higher magnification in images C-E. B. Macrophage-specific stains including HAM56 (red), CD163 (green) and calprotectin-stained neutrophils (blue). Grey line outlines the tissue edge denoted by the dashed line in A where the fibrocalcific interface has separated from the surrounding tissue and reflected over the other side. White box indicates the region depicted at higher magnification in images C-E. C. iNOS (green) and Arg1 (red) expression with nuclei (blue). D. CD68 (red) and eNOS (green) expression with nuclei (blue). E. Arg2 (green) expression with nuclei (blue). Scale bars represent 100 μm.

Figure 7.

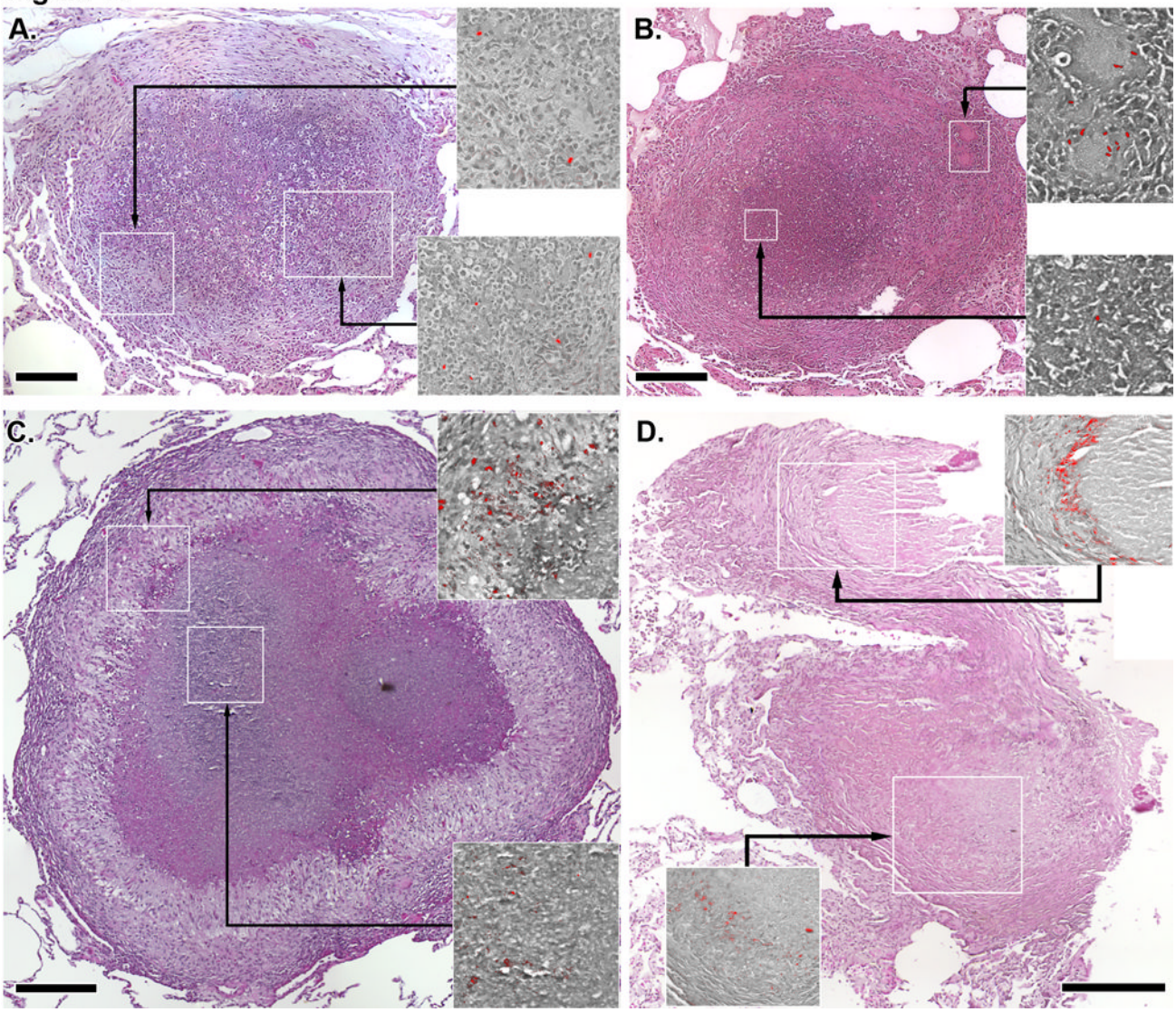

Figure 7. Bacteria and bacterial antigens can be detected in granulomas from active and latent disease

Auramine-rhodamine images (red images overlayed on grayscale hematoxylin and eosin backgrounds) indicating the presence of mycobacteria in granulomas come from regions indicated by white boxes in the colored hematoxylin and eosin-stained granuloma. Auramine-rhodamine stains come from the same tissue section as the hematoxylin and eosin-stained image. A. A necrotic granuloma with large numbers of neutrophils infiltrating into the caseum showing bacteria in epithelioid macrophages (top panel) and admixed with macrophage and neutrophils (bottom panel). B. A necrotic granuloma with bacilli in giant cells in the granuloma periphery (top panel) and in the caseum (bottom panel). C. A necrotic granuloma showing mycobacterial antigens and bacilli in epithelioid macrophages and adjacent to foamy macrophages and mycobacterial antigens in the caseum (bottom panel). D. A fibrotic granuloma from an animal with latent TB showing residual mycobacterial antigens at the interface of highly fibrotic tissue (top and bottom panels). Scale bars represent 200 μm.

Figure 8.

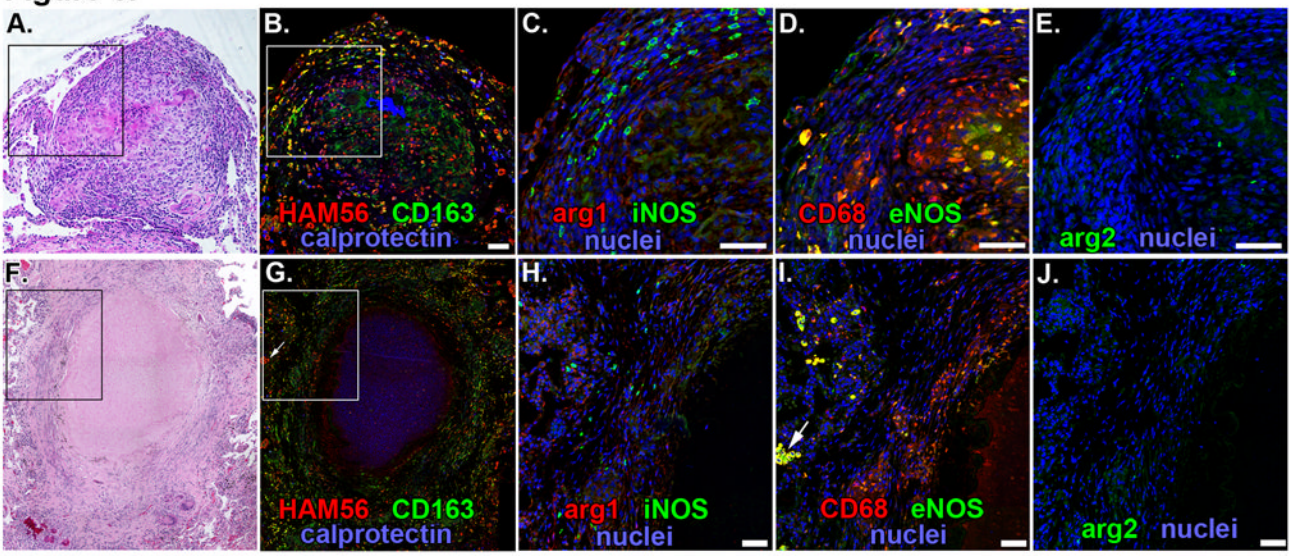

Figure 8. Macrophage phenotypes and distribution in non-necrotic and necrotic human granulomas

Panels A-E indicate images of a non-necrotic granuloma, panels F-J indicate images of a necrotic granuloma. Black boxes (hematoxylin and eosin images) and white boxes (HAM56, CD163, calprotectin images) denote areas shown in the higher magnification Arg1/iNOS, CD68/eNOS, Arg2 panels. A, F. Hematoxylin and eosin staining. B, G. Macrophage-specific stains including HAM56 (red), CD163 (green) and calprotectin-stained neutrophils (blue). C, H. iNOS (green) and Arg1 (red) expression with nuclei (blue). D, I. CD68 (red) and eNOS (green) expression with nuclei (blue). Arrows indicate clusters of CD68+eNOS+ cells adjacent to the granuloma. E, J. Arg2 (green) expression with nuclei (blue). Scale bars represent 50 μm.